Computing the Heteroclinic Orbits Splitting in Systems Phase Spaces via the Matricant Method

Anton V. Doroshin, *Member, IAENG*

***Abstract*—It is well known fact, that the heteroclinic trajectories are one of the most important elements of phase spaces of dynamical system, independently from their nature, because these trajectories separate zones of phase spaces with different dynamical behaviors. Moreover, the heteroclinic trajectories can be splitted under the action of perturbations, and can generate so-called heteroclinic nets due to intersections of splitted manifolds – this circumstance results in the chaotic dynamics creation, that, in its turn, substantially change the system dynamics. In this work a new approach for computing the heteroclinic splitting via the matricant method is developed, and also the approximate numerical technique of this method implementation is build. The example of the method application is given on the base of the spacecraft attitude dynamics.**

***Keywords*—heteroclinic trajectory, gyrostat-satellite, attitude dynamics, dynamical chaos, matricant**

I. Introduction

The nonlinear dynamics and dynamical systems theory, undoubtedly, are the fast developing parts of the modern science, which describe the dynamical behavior and time-evolutions of different systems independently from their nature (including the technical, chemical, physical, biological systems, etc.). The systems dynamics is usually analyzed in terms of phase spaces coordinates, phase trajectories and phase regions. One of the important aspect of the analysis of the systems dynamics is the investigation of the separatrixes trajectories in phase spaces, which correspond to homo-/heteroclinic phase trajectories and divide the whole phase space into some independent parts. At the action of perturbations, the homo-/heteroclinic trajectories can be splitted into the corresponding stable and unstable manifolds (without perturbations they merge into the single separatrix-trajectory). Moreover, these splitted manifolds can be mutually intersecting each other – in this case they will generate the corresponding heteroclinic nets in the phase space, that inevitably initiates the dynamical "heteroclinic" chaos which can substantially change the system's dynamics or even fully disrupt its predicted dynamical behavior. Therefore, it is so important to learn and to know the details of the process of the heteroclinic splitting. The modern methods of the exploration of the separatrixes' manifolds splitting are based on the Melnikov's-Wiggins' formalism [1-5], which was started in works of V.K. Melnikov (1963) and V.I. Arnold (1964), was alternatively interpreted in works V.V. Kozlov (1980), and was extended in works P.J. Holmes & J.E. Marsden (1983), and S. Wiggins (1988). It is worth to note, however, that this formalism is well and correctly applicable for homoclinic separatrixes, but has some difficulties at the analysis of the heteroclinic splitting [6].

So, in the purposes of the alternative method developing, which can be correctly applied to any cases of the separatrixes splitting analysis (both homo- and heteroclinic cases), we must, firstly, construct the analytical procedure of the splitted manifolds calculation and, secondly, have to adopt this analytical procedure to its numerical implementation.

Manuscript received December 3, 2017. This work is supported by the Ministry of education and science of the Russian Federation in the framework of the design part of the State Assignments to higher education institutions and research organizations in the field of scientific activity - the project #9.1616.2017/ПЧ (9.1616.2017/4.6).

A. V. Doroshin is with the Space Engineering Department (Division of Flight Dynamics and Control Systems), Samara National Research University (SSAU, 34, Moskovskoe Shosse str., Samara, 443086, Russia; e-mail: doran@inbox.ru; doroshin@ssau.ru); IAENG Member No: 110131.

II. Images of Splitted Manifolds of the Perturbed Heteroclinic Trajectory

Let us to consider the dynamical system describing by the ordinal differential equations $\left(\mathbf{x}\in\mathbb{R}^N\right)$:

$$\begin{aligned}\dot{\mathbf{x}}&=\mathbf{F}\left(\mathbf{x}\right)+\varepsilon\mathbf{f}\left(\mathbf{x},t\right)\\ \mathbf{x}&=\left\{x_1\left(t\right),...,x_n\left(t\right)\right\}^T\end{aligned}\tag{1}$$

where ε is the small parameter, $\mathbf{f}$ is the perturbing function.

We assume, that the system (1) in the unperturbed case (ε=0) has the heteroclinic trajectories, which are known in the shape of exact explicit analytical solutions:

$$\bar{\mathbf{x}}=\bar{\mathbf{x}}\left(t\right)=\left\{\bar{x}_1\left(t\right),...,\bar{x}_n\left(t\right)\right\}^T\tag{2}$$

The solution of the perturbed system (1) we will find in the neighborhood of one of the heteroclinic trajectories (2) in the form:

$$\mathbf{x}\left(t\right)=\bar{\mathbf{x}}\left(t\right)+\varepsilon\mathbf{X}\left(t\right)\tag{3}$$

After substituting (3) into the equations (1) and after linearization by the small parameters, we obtain the equations of the first order for deviations $\mathbf{X}(t)$:

$$\dot{\mathbf{X}}=\mathbf{S}\left(\bar{\mathbf{x}}\left(t\right)\right)\cdot\mathbf{X}+\mathbf{f}\left(\bar{\mathbf{x}}\left(t\right),t\right)\tag{4}$$

where $\mathbf{S}$ is the known functional matrix N×N.

In the purposes of the heteroclinic splitting analysis, we have to solve the deviations system (4) for each point of each splitted manifolds (starting from the points of the unperturbed heteroclinic trajectory) on the interval of the physical time $t\in[0,T]$, and then the obtained solutions allow us to detect all possible intersections of the whole splitted manifolds in the time-point T.

ISBN: 978-988-14047-8-7
ISSN: 2078-0958 (Print); ISSN: 2078-0966 (Online)

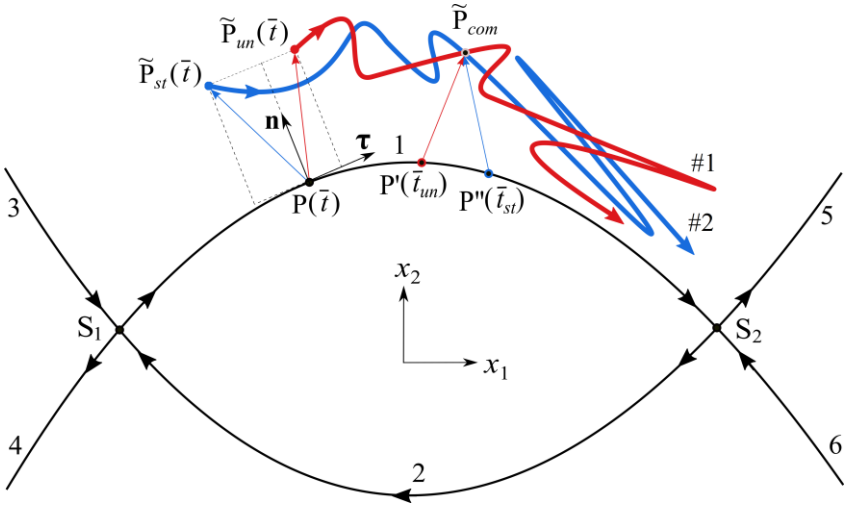

Fig.1. The heteroclinic splitting structure and the heteroclinic net as the set of the Poincaré-images of the unperturbed trajectory (the color version is available only in the online article)

As it is customary for the majority of the research works, the heteroclinic splitting usually is considered under the action of the time-periodic perturbations **f**. In such cases the perturbed dynamics is studied with the help of the well-known Poincaré sections methodology, when the phase space is considered in the "stroboscopic" regime; i.e. the phase trajectories are depicted in the phase space as sets of their discrete points corresponding to the discrete physical *t*-time values, which are multiple to the perturbation period *T*, when $\mathrm{mod}(t, 2\pi/\Omega) = 0$. Therefore, for each phase point of the phase space $\mathbf{x} \in \mathbb{R}^N$ we will see its image, which is calculated by the Poincaré map (let us assume temporarily that χ =1):

$$\wp_i : \ \mathbf{x}_0(\bar{t}) \to \mathbf{x}(\bar{t}+T); \qquad T = \frac{2\pi i}{\Omega}\chi; \quad t_i = 2\pi i \chi/\Omega \tag{5}$$

If we focus separately on the heteroclinic separatrix, then we also will see its perturbed manifolds as the images of all its points by the map (5): the unstable manifolds will correspond to the direct forward images of its points (at steps of the map in the positive direction of the physical time, where *i* >0), and the stable manifold will correspond to the first preimages of the separatrix's points (at steps of the map in the opposite/negative direction of the physical time, where *i* <0). So, in each separated "stroboscopic" time-point (in each step of the Poincaré map) we will see the "independent" evolution of each phase-point of the unperturbed separatrix – together these images form the shape of the whole heteroclinic splitted manifold. Moreover, the first image $(i=1;\ T=2\pi\chi/\Omega)$ and the first preimage $(i=-1;\ T=-2\pi\chi/\Omega)$ are the most important frames to our dynamical analysis, because exactly on these frames the main (the first) shapes of the perturbed manifolds are presented; and exactly these shapes will generate all next images|preimages of the manifolds.

At the fig.1 two saddle-points S_1 and S_2 form two heteroclinic trajectories: S_1S_2 – the branch 1 and S_2S_1 – the branch 2, and also these saddle-points have free branches (the branches 3-6). As it is clear, the branch 1 represents the merger of the unstable manifold of the S_1–saddle and the stable manifold of the S_2–saddle. Under the action of perturbations these manifolds split into separate trajectories, that is depicted at the fig.1: the curve #1 (the red curve) corresponds to the splitted unstable manifold of the S_1–saddle (it is the first Poincaré-map image of all points of the unperturbed trajectory S_1S_2 at *i*=1), and the curve #2 (the blue curve) - to the splitted stable manifold of the S_2–saddle (it is the first Poincaré-map preimage of all points of the unperturbed trajectory S_1S_2 at *i*=-1).

If we know the analytical exact explicit solutions for the heteroclinic trajectory, then the concrete point P on the unperturbed branch 1 can be parameterized by the parameter $\bar{t}$ (the time of the parameterization). Vectors **n** and **τ** are the normal and transversal vectors for the heteroclinic trajectory at the point $\mathrm{P}(\bar{t})$, which is "sliding" along trajectory at the parameter $\bar{t}$ changing. The first image of this point $\mathrm{P}(\bar{t})$ is presented at the fig.1 as the point $\tilde{\mathrm{P}}_{un}(\bar{t})$ - this point belong to the splitted unstable manifold of the S_1–saddle. The first preimage of this point $\mathrm{P}(\bar{t})$ is presented at the fig.1 as the point $\tilde{\mathrm{P}}_{st}(\bar{t})$ - this point belong to the splitted stable manifold of the S_2–saddle. So, the points $\tilde{\mathrm{P}}_{un}(\bar{t})$ and $\tilde{\mathrm{P}}_{st}(\bar{t})$ formally correspond to the perturbed positions of one and the same point $\mathrm{P}(\bar{t})$. From the case depicted at the fig.1 it is possible to see, that these images can have the same distances relative the unperturbed point $\mathrm{P}(\bar{t})$ along normal direction **n**:

$$\left[\overrightarrow{\mathrm{P}(\bar{t})\tilde{\mathrm{P}}_{un}(\bar{t})}\cdot\mathbf{n}\right] = \left[\overrightarrow{\mathrm{P}(\bar{t})\tilde{\mathrm{P}}_{st}(\bar{t})}\cdot\mathbf{n}\right] \tag{6}$$

but different distances along the transversal direction **τ**:

$$\left[\overrightarrow{\mathrm{P}(\bar{t})\tilde{\mathrm{P}}_{un}(\bar{t})}\cdot\boldsymbol{\tau}\right] \neq \left[\overrightarrow{\mathrm{P}(\bar{t})\tilde{\mathrm{P}}_{st}(\bar{t})}\cdot\boldsymbol{\tau}\right] \tag{7}$$

From the point of view of the Melnikov's method, the condition (6) in the linear approximation defines the fact of the intersection of splitted manifolds independently from the fulfillment/non-fulfillment of the expression (7); i.e. the Melnikov function will have the zero-value in this case. At the same time, in the depicted case the real intersection of the splitted manifolds, as we see, does not occur.

ISBN: 978-988-14047-8-7
ISSN: 2078-0958 (Print); ISSN: 2078-0966 (Online)

Moreover, the real intersection of the splitted manifolds can be occurred for different "sliding" unperturbed points P' and P" (fig.1) – the image of the point P' coincides with the preimage of the point P" in the common perturbed point $\tilde{\mathrm{P}}_{com}$. For this reason, it will be appropriate to introduce into the consideration two separated parameters of the heteroclinic trajectory parameterization instead of the single parameter $\bar{t}$. Therefore, to parameterize the unstable manifolds we will use the parameter $\bar{t}_{un}$ "sliding" along the unperturbed heteroclinic trajectory; and for parameterization of the stable manifold we introduce the "sliding" parameter $\bar{t}_{st}$.

So, our main task now is to obtain the solutions for the deviations $\mathbf{X}(T)$ for the each unperturbed point (like P) of heteroclinic trajectory for all system's heteroclinic trajectories and theirs splitted stable and unstable manifolds – then we can see the all possible intersections of all splitted manifolds (like $\tilde{\mathrm{P}}_{com}$).

III. The Exact Computation of the Images of the Splitted Manifolds of the Heteroclinic Trajectory

Now we can find the deviation of each point of the heteroclinic trajectory (e.g., P) at its splitting into the unstable and stable manifolds (at the physical time point $\pm T$) by the integrating of the differential equations (4) in the direct time direction for the unstable manifold and in the back time direction for the stable manifold, starting in all cases from the points of the heteroclinic trajectory (i.e. at the zero-values of initial conditions $\mathbf{X}(0)=0$).

For our task of solving the linear differential equations (4) with the time-depending coefficients $\left(\mathbf{S}\left(\bar{\mathbf{x}}(t)\right)\right)$, the classical form of the solution is known, which uses the matricant-object [e.g., 7]:

$$\mathbf{X}(t)=\mathbf{\Omega}_{t_0}^{t}\left(\mathbf{S}\left(\bar{\mathbf{x}}(t)\right)\right)\cdot\int_{t_0}^{t}\left\{\left[\mathbf{\Omega}_{t_0}^{\tau}\left(\mathbf{S}\left(\bar{\mathbf{x}}(\tau)\right)\right)\right]^{-1}\cdot\mathbf{f}\left(\bar{\mathbf{x}}(\tau),\tau\right)\right\}d\tau \quad (8)$$

where $\mathbf{\Omega}_{t_0}^{t}\left(\mathbf{S}(t)\right)$ is the so-called *matricant*, which can be evaluated by the following ways [7]:

$$\begin{aligned}\mathbf{\Omega}_{t_0}^{t}\left(\mathbf{S}(t)\right)&=\mathbf{E}+\int_{t_0}^{t}\mathbf{S}(t)\,dt+\int_{t_0}^{t}\mathbf{S}(t)\left[\int_{t_0}^{t}\mathbf{S}(t)\,dt\right]dt+\\&+\int_{t_0}^{t}\mathbf{S}(t)\left[\int_{t_0}^{t}\mathbf{S}(t)\left[\int_{t_0}^{t}\mathbf{S}(t)\,dt\right]dt\right]dt+\ldots\end{aligned} \quad (9)$$

$$\begin{aligned}\mathbf{\Omega}_{t_0}^{t}\left(\mathbf{S}(t)\right)=\lim_{\substack{\Delta t_k\to 0\\ n\to\infty}}&\left\{\left[\mathbf{E}+\mathbf{S}(\tau_n)\Delta t_n\right]\cdot\ldots\cdot\right.\\&\left.\cdot\left[\mathbf{E}+\mathbf{S}(\tau_2)\Delta t_2\right]\cdot\left[\mathbf{E}+\mathbf{S}(\tau_1)\Delta t_1\right]\right\}\end{aligned} \quad (10)$$

Here $\mathbf{E}$ – is the identity matrix; and in the form (10) the idea is used, that the time-interval $[t_0, t]$ is divided on n subintervals, Δt_k is the length of the k-th subinterval and τ_k is an internal point of the k-th subinterval. We ought additionally to say, that in the form (10) the expression under the limit is called as the "integral multiplication"; and the limit itself – is called as the "multiplicative integral". From the definition of the matricant the important property follows:

$$\mathbf{\Omega}_{t_0}^{t}\left(\mathbf{S}(t)\right)=\mathbf{\Omega}_{t_{n-1}}^{t}\left(\mathbf{S}(t)\right)\cdot\ldots\cdot\mathbf{\Omega}_{t_1}^{t_2}\left(\mathbf{S}(t)\right)\cdot\mathbf{\Omega}_{t_0}^{t_1}\left(\mathbf{S}(t)\right) \quad (11)$$

So, at the "final" time $t=t_k=T$ the solution (8) formally will represent the deviation of one point of the separatrix, which was parameterized by the zero-value of sliding parameters $\left(\bar{t}=0\right)$; and therefore, to write the solution for all possible deviations of the points of the separatrix, we must explicitly involve the sliding parameters. Moreover, the system (4) and the solution (8) were configured for the direct time (the differentiation/integration in the forward time-direction). Taking here the local conclusion, we can write the solutions for the points of the splitted unstable manifold:

$$\begin{aligned}&\mathbf{X}_{un}\left(\bar{t}_{un}+T\right)=\mathbf{\Omega}_0^{T}\left(\mathbf{S}\left(\bar{\mathbf{x}}\left(t+\bar{t}_{un}\right)\right)\right)\cdot\\&\cdot\int_0^{T}\left\{\left[\mathbf{\Omega}_0^{\tau}\left(\mathbf{S}\left(\bar{\mathbf{x}}\left(\tau+\bar{t}_{un}\right)\right)\right)\right]^{-1}\cdot\mathbf{f}\left(\bar{\mathbf{x}}\left(\tau+\bar{t}_{un}\right),\tau\right)\right\}d\tau\end{aligned} \quad (12)$$

The solution (12) gives the deviation of the point $\mathrm{P}\left(\bar{t}_{un}\right)$ of the unstable manifold at the value of the physical time $t=T$. The coordinates of the first image $\tilde{\mathrm{P}}_{un}\left(\bar{t}_{un}\right)$ of the point $\mathrm{P}\left(\bar{t}_{un}\right)$ belonging to the unstable manifold and calculated by the Poincaré map (5) can be written using (3):

$$\mathbf{x}_{un}\left(\bar{t}_{un}+T\right)=\bar{\mathbf{x}}\left(\bar{t}_{un}+T\right)+\varepsilon\mathbf{X}_{un}\left(\bar{t}_{un}+T\right) \quad (13)$$

To obtain more convenience shape of expressions (13) and (12), we can simply redefine the sliding parameter by the shift on the constant T:

$$\bar{t}_{un}\leftarrow\left(\bar{t}_{un}-T\right) \quad (14)$$

The expressions (13) and (12) will have the following form:

$$\begin{cases}\mathbf{x}_{un}\left(\bar{t}_{un}\right)=\bar{\mathbf{x}}\left(\bar{t}_{un}\right)+\varepsilon\mathbf{X}_{un}\left(\bar{t}_{un}\right);\\[2ex]\mathbf{X}_{un}\left(\bar{t}_{un}\right)=\mathbf{\Omega}_0^{T}\left(\mathbf{S}\left(\bar{\mathbf{x}}\left(t-T+\bar{t}_{un}\right)\right)\right)\cdot\\\cdot\int_0^{T}\left\{\left[\mathbf{\Omega}_0^{\tau}\left(\mathbf{S}\left(\bar{\mathbf{x}}\left(\tau-T+\bar{t}_{un}\right)\right)\right)\right]^{-1}\cdot\mathbf{f}\left(\bar{\mathbf{x}}\left(\tau-T+\bar{t}_{un}\right),\tau\right)\right\}d\tau\end{cases} \quad (15)$$

To obtain the values of the phase coordinates of the first (pre)images of points of the stable manifold (at the value of the physical time $t=-T$), we formally must repeat all the above indicated steps, but at the change the physical time-variable on its opposite direction $\left(t\leftarrow(-t),\ dt\leftarrow(-dt)\right)$ and at the redefinition of sliding parameter $\left(\bar{t}_{st}\leftarrow\left(\bar{t}_{st}+T\right)\right)$.

Then we can write:

$$\begin{cases}\mathbf{x}_{st}\left(\bar{t}_{st}\right)=\bar{\mathbf{x}}\left(\bar{t}_{st}\right)+\varepsilon\mathbf{X}_{st}\left(\bar{t}_{st}\right);\\[2ex]\mathbf{X}_{st}\left(\bar{t}_{st}\right)=\mathbf{\Omega}_0^{T}\left(-\mathbf{S}\left(\bar{\mathbf{x}}\left(\bar{t}_{st}-t+T\right)\right)\right)\cdot\\\cdot\int_0^{T}\left\{\left[\mathbf{\Omega}_0^{\tau}\left(-\mathbf{S}\left(\bar{\mathbf{x}}\left(\bar{t}_{st}-\tau+T\right)\right)\right)\right]^{-1}\cdot(-1)\mathbf{f}\left(\bar{\mathbf{x}}\left(\bar{t}_{st}-\tau+T\right),-\tau\right)\right\}d\tau\end{cases} \quad (16)$$

Now let us remind the value χ in the map (5): if $\chi=1$ then the Poincaré map corresponds to the classical "periodical" form; another value for this parameter scales the map's steps. As it was noted, the first step is most important for the problem of manifolds spliting, and, therefore, the value χ allow to correct the "length" of this step, that extends the applicability of expressions (15) and (16) on an arbitrary value of the physical time-point T (from nil to infinity).

So, the expressions (15) and (16) represent the exact analytical solutions of the first order-system (4) for the

ISBN: 978-988-14047-8-7
ISSN: 2078-0958 (Print); ISSN: 2078-0966 (Online)

splitted manifolds of the heteroclinic trajectory at the action of perturbations for the arbitrary time-point *T*.

The separated question connects here with difficulties of the analytical computation of the matricant, so we have to construct the procedure of numerical calculations of the obtained solutions (15) and (16), that will be realize in the next section.

IV. The Numerical Computation of Images of the Splitted Manifolds of the Heteroclinic Trajectory

Now using the analytical forms of the solutions (15) and (16), we can construct the procedure to numerical calculations of the splitted manifolds of the heteroclinic trajectories with an arbitrarily accurate.

The basic numerical procedure we will synthesize for the case of the action of high-frequency harmonic perturbations, when the period is small ($T<<1$) or for the case when the step of the map (5) is scaled by the small value $\chi<<1$. Then, starting from the form of harmonic periodic perturbation, we will consider four even more small quarter-period-subintervals for the physical time:

$$t\in[0..T]=\left[[0..T/4],[T/4..T/2],[T/2..3T/4],[3T/4..T]\right].$$

It is possible to formally write the structure of the integral it the right part (15) and (16) using the well-known Simpson's rule of numerical integration on two half-period-subintervals (i.e. each Simpson-step covers two corresponding quarter-period-subintervals):

$$\begin{aligned}\hat{\mathbf{I}}(\bar{t})&=\int_0^T\left\{\left[\mathbf{\Omega}_0^{\tau}\left(\hat{\mathbf{S}}(\bar{t},\tau)\right)\right]^{-1}\cdot\hat{\mathbf{f}}(\bar{t},\tau)\right\}d\tau=\\&=\frac{T}{12}\left\{\mathbf{E}\cdot\hat{\mathbf{f}}(\bar{t},0)+4\left[\hat{\mathbf{\Omega}}_0^{T/4}\right]^{-1}\cdot\hat{\mathbf{f}}\left(\bar{t},\frac{T}{4}\right)+\right.\\&+2\left[\hat{\mathbf{\Omega}}_0^{T/2}\right]^{-1}\cdot\hat{\mathbf{f}}\left(\bar{t},\frac{T}{2}\right)+4\left[\hat{\mathbf{\Omega}}_0^{3T/4}\right]^{-1}\cdot\hat{\mathbf{f}}\left(\bar{t},\frac{3T}{4}\right)+\\&\left.+\left[\hat{\mathbf{\Omega}}_0^{T}\right]^{-1}\cdot\hat{\mathbf{f}}(\bar{t},T)\right\}\end{aligned}\tag{17}$$

where for convenience and in order to unify the shape of the result for both cases (*un*, *st*) the following notations were involved:

$$\begin{cases}\hat{\mathbf{S}}(\bar{t},\tau)=\begin{cases}\mathbf{S}\left(\bar{\mathbf{x}}\left(\tau-T+\bar{t}_{un}\right)\right), & \text{in the case "}un\text{"}\\-\mathbf{S}\left(\bar{\mathbf{x}}\left(\bar{t}_{st}-\tau+T\right)\right), & \text{in the case "}st\text{"}\end{cases}\\\hat{\mathbf{f}}(\bar{t},\tau)=\begin{cases}\mathbf{f}\left(\bar{\mathbf{x}}\left(\tau-T+\bar{t}_{un}\right),\tau\right), & \text{in the case "}un\text{"}\\-\mathbf{f}\left(\bar{\mathbf{x}}\left(\bar{t}_{st}-\tau+T\right),-\tau\right), & \text{in the case "}st\text{"}\end{cases}\end{cases}\tag{18}$$

$$\begin{cases}\hat{\mathbf{\Omega}}_0^{T/4}=\mathbf{E}+\hat{\mathbf{S}}(\bar{t},0)\cdot\frac{T}{4}\\\hat{\mathbf{\Omega}}_0^{T/2}=\left(\mathbf{E}+\hat{\mathbf{S}}\left(\bar{t},\frac{T}{4}\right)\cdot\frac{T}{4}\right)\cdot\hat{\mathbf{\Omega}}_0^{T/4}\\\hat{\mathbf{\Omega}}_0^{3T/4}=\left(\mathbf{E}+\hat{\mathbf{S}}\left(\bar{t},\frac{T}{2}\right)\cdot\frac{T}{4}\right)\cdot\hat{\mathbf{\Omega}}_0^{T/2}\\\hat{\mathbf{\Omega}}_0^{T}=\left(\mathbf{E}+\hat{\mathbf{S}}\left(\bar{t},\frac{3T}{4}\right)\cdot\frac{T}{4}\right)\cdot\hat{\mathbf{\Omega}}_0^{3T/4}\end{cases}\tag{19}$$

where the designation of the matricant $\hat{\mathbf{\Omega}}_0^{\tau}=\mathbf{\Omega}_0^{\tau}\left(\hat{\mathbf{S}}(\bar{t},\tau)\right)$ also combines both cases (*un*, *st*) through the choice of corresponding shape (18) of the matrix $\hat{\mathbf{S}}(\bar{t},\tau)$.

Here we ought to note, that the expressions (19) were approximately obtained from the main definition of the matricant (10) considering the property (11). At the any preassigned values of sliding parameters $\bar{t}=\left\{\bar{t}_{un}\ \text{or}\ \bar{t}_{st}\right\}$ the expressions (19) immediately receive their numerical matrix values.

The expressions (17)-(19) fully define the numerical values of points coordinates of the images of the perturbed splitted manifolds for all values of sliding parameters $\left(\hat{\mathbf{x}}(\bar{t})=\left\{\mathbf{x}_{un}(\bar{t}_{un})\ \text{or}\ \mathbf{x}_{st}(\bar{t}_{st})\right\};\ \hat{\mathbf{X}}(\bar{t})=\left\{\mathbf{X}_{un}(\bar{t}_{un})\ \text{or}\ \mathbf{X}_{st}(\bar{t}_{st})\right\}\right)$:

$$\hat{\mathbf{x}}(\bar{t})=\bar{\mathbf{x}}(\bar{t})+\varepsilon\hat{\mathbf{X}}(\bar{t});\qquad\hat{\mathbf{X}}(\bar{t})=\hat{\mathbf{\Omega}}_0^{T}\cdot\hat{\mathbf{I}}(\bar{t})\tag{20}$$

So, now we have constructed the procedure of numerical computing the splitted manifolds of the heteroclinic trajectories. Certainly, the formulae (20) represent the approximate numerical solutions; and, of course, expressions that are more precise can be built on the basis of exact explicit analytical solutions (15) and (16).

V. An Example of the Calculation of the Splitted Heteroclinic Manifolds in the Task of Gyrostats Perturbed Dynamics

Let us now to implement the obtained scheme of the calculation of the splitted manifolds (their images) of the heteroclinic trajectories in the framework of the task of the torque-free one-rotor gyrostat motion [6]. The main dynamical system of the torque-free one-rotor gyrostat can be found in many works, e.g. in [6]:

$$\begin{cases}A\dot{p}+(C_b-B)qr+q\Delta=0;\ \ B\dot{q}+(A-C_b)pr-p\Delta=0;\\C_b\dot{r}+\dot{\Delta}+pq(B-A)=0;\qquad\dot{\Delta}=M_{internal}\end{cases}\tag{21}$$

where $A=A_b+A_r$, $B=B_b+A_r$; and $\{A_b,B_b,C_b\}$ correspond to the axial inertia moments of the main SC body in the connected frame; and $\{A_r,A_r,C_r\}$ represent the axial inertia moments of the dynamically symmetrical rotor in its own connected frame; $[p,\ q,\ r]^T$ – are components of the vector of the angular velocity of the main body in the connected frame, σ – is the angular velocity of the rotor rotation relative the main body; $\Delta=C_r(r+\sigma)$- is the angular momentum of the rotor-body, which is rotated around the general longitudinal axis of the main body.

If $M_{internal}$=0 then the unperturbed motion realizes, and then the phase space represents so-called polhode-ellipsoids in the 3D-space $\mathbf{x}=[p,q,r]^T\in\mathbb{R}^3$ (fig.2).

For this system in some important dynamical cases, the heteroclinic solutions are known [6], and for the torque-free motion this analytical solutions are the following:

$$\bar{\mathbf{x}}(\bar{t})=\left[\bar{p}(\bar{t}),\bar{q}(\bar{t}),\bar{r}(\bar{t})\right]^T;$$

$$\begin{cases}\bar{p}(\bar{t})=\pm\sqrt{\frac{C_b(B-C_b)}{A(A-B)}}\xi(\bar{t});\\\bar{q}(\bar{t})=\pm\sqrt{\varsigma^2-\vartheta^2\left(\xi(\bar{t})+\bar{\Delta}\beta\right)^2};\\\bar{r}(\bar{t})=\xi(\bar{t})+\frac{\bar{\Delta}}{B-C_b};\end{cases}\tag{22}$$

where

ISBN: 978-988-14047-8-7
ISSN: 2078-0958 (Print); ISSN: 2078-0966 (Online)

$$\xi(\bar{t}) = \frac{4a_0\Phi_0 \exp\left(\mp\frac{\tilde{M}\sqrt{a_0}}{\vartheta^2}\bar{t}\right)}{\left[\Phi_0 \exp\left(\mp\frac{\tilde{M}\sqrt{a_0}}{\vartheta^2}\bar{t}\right) - a_1\right]^2 - 4a_2a_0}$$

with the set of constants:

$$\begin{cases} \bar{\Delta} = \text{const} > 0; \quad a_2 = -\vartheta^2; \quad a_1 = -2\bar{\Delta}\beta\vartheta^2; \\ a_0 = \varsigma^2 - \vartheta^2\bar{\Delta}\beta^2; \quad \varsigma^2 = \dfrac{\tilde{H}}{B(A-B)}; \\ \vartheta^2 = \dfrac{C_b(A-C_b)}{B(A-B)}; \quad \tilde{M} = \dfrac{(A-C_b)}{B}\sqrt{\dfrac{C_b(B-C_b)}{A(A-B)}}; \\ \tilde{H} = 2\tilde{T}\left(A-\tilde{D}\right) + \dfrac{C_b}{A-C_b}\bar{\Delta}^2 - \left(\dfrac{A}{C_r}-1\right)\bar{\Delta}^2; \\ \tilde{D} = B + \dfrac{1}{2\tilde{T}}\left(\dfrac{C_b}{B-C_b}\bar{\Delta}^2 - \left(\dfrac{B}{C_r}-1\right)\bar{\Delta}^2\right); \\ \tilde{T} = T_0; \quad 2T_0 = Ap_0^2 + Bq_0^2 + C_br_0^2 + \dfrac{\bar{\Delta}^2}{C_r}; \\ \Phi(z) = \dfrac{1}{z}\left(2a_0 + a_1z + 2\sqrt{a_0}\sqrt{a_2z^2 + a_1z + a_0}\right); \\ \Phi_0 = \Phi\left(y_0^{\pm}\right); \; y_0^{\pm} = \pm\dfrac{\varsigma}{\vartheta} - \bar{\Delta}\beta; \; \beta = \dfrac{A-B}{(B-C_b)(A-C_b)} \end{cases}$$

The analytical solutions (22) describe four heteroclinic trajectories connecting the saddle-points S_1 and S_2 (fig.2). Here we can note, that the heteroclinic scheme presented at the fig.1 in the case of the torque-free gyrostat will have two closed heteroclinic loops connecting by four corresponding branches ({3, 5} and {4, 6} as at the fig.1) – it doubles the quantity of heteroclinic trajectories, that even more complicates the analysis of heteroclinic splitting.

Now let us consider the small ($\mu_\Delta << 1$) periodic internal perturbation in the rotor-spinup-engine, which is described by the small torque:

$$M_{internal} = \mu_\Delta \cos(\omega_\Delta t) \tag{23}$$

Then the solution for the rotor's angular momentum follows:

$$\Delta(t) = \bar{\Delta} + \frac{\mu_\Delta}{\omega_\Delta}\sin(\omega_\Delta t) \tag{24}$$

The substitution of the solution (24) into the equations (21) gives the perturbed system:

$$\begin{cases} A\dot{p} + (C_b - B)qr + q\bar{\Delta} = -\varepsilon C_b\omega_\Delta \sin(\omega_\Delta t)q; \\ B\dot{q} + (A - C_b)pr - p\bar{\Delta} = \varepsilon C_b\omega_\Delta \sin(\omega_\Delta t)p; \\ C_b\dot{r} + pq(B-A) = -\varepsilon C_b\omega_\Delta^2 \cos(\omega_\Delta t), \end{cases} \tag{25}$$

where the small dimensionless parameter is involved

$$\varepsilon = \frac{\mu_\Delta}{C_b\omega_\Delta^2} \tag{26}$$

In the considered case, we have the following coefficients matrix and the perturbing function for the linearized perturbed system (4) $\left(\mathbf{X} = [P, Q, R]^T\right)$:

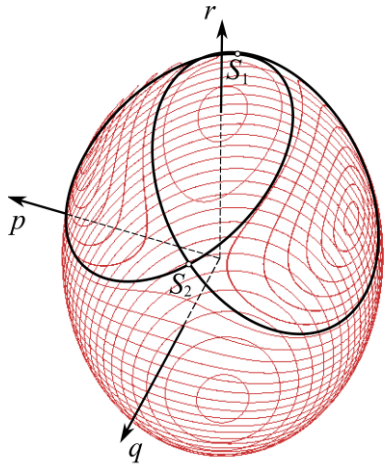

Fig.2. The gyrostat's phase space and the heteroclinic trajectories

$$\mathbf{S}(\bar{\mathbf{x}}) = \begin{bmatrix} 0 & -\dfrac{\left((C_b-B)\bar{r}+\bar{\Delta}\right)}{A} & -\dfrac{(C_b-B)\bar{q}}{A} \\ -\dfrac{\left((A-C_b)\bar{r}-\bar{\Delta}\right)}{B} & 0 & -\dfrac{(A-C_b)\bar{p}}{B} \\ -\bar{q}(B-A)/C_b & -\bar{p}(B-A)/C_b & 0 \end{bmatrix} \tag{27}$$

$$\mathbf{f}(\bar{\mathbf{x}}, t) = C_b\omega_\Delta^2 \begin{bmatrix} \dfrac{-\bar{q}\sin(\omega_\Delta t)}{A\omega_\Delta} \\ \dfrac{\bar{p}\sin(\omega_\Delta t)}{B\omega_\Delta} \\ -\dfrac{\cos(\omega_\Delta t)}{C_b} \end{bmatrix} \tag{28}$$

So, using expressions (17)-(20) and having the heteroclinic solutions (22), we can numerically calculate the images of the splitted manifolds of the heteroclinic branch for the system (25) (and its corresponding linearization (4) with the matrix- and vector-functions (27), (28)). The corresponding numerical calculation was implemented – the corresponding numerical results are depicted at the figures (fig.3-fig.5). The splitted manifolds of the branch 1 are presented at the fig.3, where the image of the unstable perturbed manifold depicted as the set #1 of points (red points), and the (pre)image of perturbed stable manifolds represent the set #2 of points (blue points). Small points at the fig.3 correspond to the direct integration results of the equations (25) on the time-interval [0, T] for the set of initial points on the unperturbed branch; and the big points – are the points calculated by the matricant method (20). As we can see, the integration results and results calculated by the matricant method coincide with each other with the good consistency – this confirms the operability of the matricant method. Here we must note that the calculations (fig.3, 4, 5) were implemented at the following system's parameters and main initial conditions, defined the unperturbed heteroclinic branch: A_r=5, C_r=4, A_b=15, B_b=8, C_b=6 [kg*m^2]; μ_Δ=120 [N*m]; ω_Δ=20 [1/s]; χ=1; T=0.3146 [s]; ε=0.05; p_0=3.5, q_0=0, r_0=6.96, σ_0=-5.96 [1/s]; Δ_0=4 [kg*m^2/s].

ISBN: 978-988-14047-8-7
ISSN: 2078-0958 (Print); ISSN: 2078-0966 (Online)

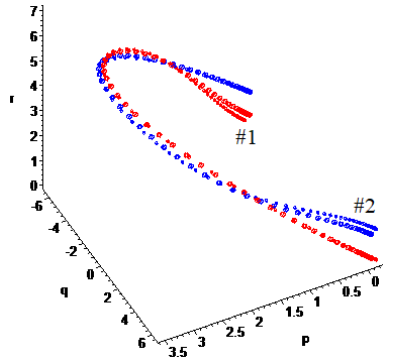

Fig.3. The splitted manifolds of the first heteroclinic branch (the color version is available only in the online article)

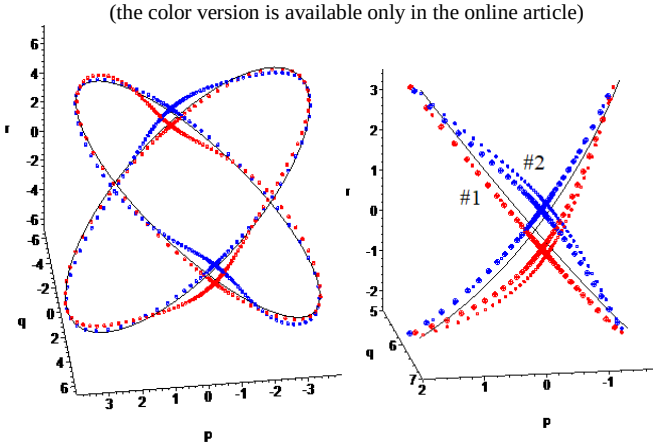

(a) (b)

Fig.4. The splitted manifolds of all four heteroclinic branches (a) and the zoom of the area of root intersections (b): the small points – the direct integrations, the big points – the results obtained by the matricant method (the color version is available only in the online article)

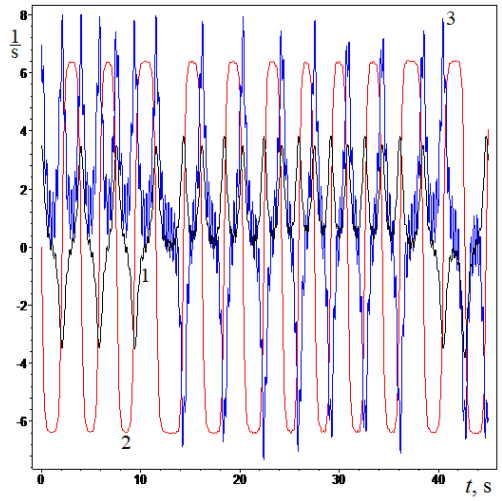

Fig.5. The chaotic time-history of the angular velocities {p, q, r} due to the realization of the heteroclinic chaos in the neighborhood of the first heteroclinic branch (p – black (1); q – red (2); r – blue (3)) (the color version is available only in the online article)

As we see from the modeling results, the intersections of the splitted manifolds take place, and, moreover, these intersections can be between the splitted manifolds of one the same branch (fig.3), and also they can be between the splitted manifolds of different branches (fig.4). This circumstance defines the presence of a complex structure of the heteroclinic net, which arises in the phase space at the action of perturbations, and which results in the chaotic dynamics, that is presented as the chaotic time-history of angular velocity components (fig.5).

VI. The Function of Detecting the Intersections of Splitted Manifolds of Heteroclinic Bundles

Now basing on the analytical expressions (15) and (16) we can construct the exact analytical vector-function for the calculation of distances between the splitted stable manifold of the *i*-th heteroclinic branch any the splitted unstable manifold of the *j*-th heteroclinic branch (for one the same branch the number *i* is equal *j*):

$$\mathbf{d}_{ij}\left(\bar{t}_{st}^{\langle i\rangle},\bar{t}_{un}^{\langle j\rangle}\right)=\mathbf{x}_{st}^{\langle i\rangle}\left(\bar{t}_{st}^{\langle i\rangle}\right)-\mathbf{x}_{un}^{\langle j\rangle}\left(\bar{t}_{un}^{\langle j\rangle}\right) \qquad (29)$$

Obviously, if the vector-function (29) has the zero-vector value at some specific values of the parameters $\left(\bar{t}_{st}^{\langle i\rangle}=\tilde{\bar{t}}_{st}^{\langle i\rangle},\ \bar{t}_{un}^{\langle j\rangle}=\tilde{\bar{t}}_{un}^{\langle j\rangle}\right)$ then the intersection/contact of these splitted manifolds exists. As we have already sad, the different branches' splitted manifolds can be intersected, and, therefore, we must browse all possible variants of the branches combinations. Then the zero-values of the following generalized scalar function $D\in\mathbb{R}^{2n}$ will show the intersections/contacts presence between splitted manifolds:

$$D\left(\bar{t}_{st}^{\langle 1\rangle},...,\bar{t}_{st}^{\langle n\rangle},\bar{t}_{un}^{\langle 1\rangle},...,\bar{t}_{un}^{\langle n\rangle}\right)=\prod_{i=1}^{n}\prod_{j=i}^{n}\left\|\mathbf{d}_{ij}\left(\bar{t}_{st}^{\langle i\rangle},\bar{t}_{un}^{\langle j\rangle}\right)\right\| \qquad (30)$$

where *n* is the quantity of the connected heteroclinic branches (e.g., in the considered task of the perturbed attitude dynamics of gyrostats *n*=4). We ought to note that the partial case of the function (29) (or (30)) can be considered in the role of the well-known Melnikov's function $M\left(\bar{t}\right)\in\mathbb{R}$ in the framework of the homoclinic loop analysis (at the single homoclinic branch, when *n*=1):

$$M\left(\bar{t}\right)\leftrightarrow\left\|\mathbf{d}\left(\bar{t}_{st}^{\langle 1\rangle},\bar{t}_{un}^{\langle 1\rangle}\right)\right\|,\quad \bar{t}_{st}^{\langle 1\rangle}=\bar{t}_{un}^{\langle 1\rangle}=\bar{t}$$

It is clear, that for numerical computing functions **d** and *D* and for the detection of their zeros we can use the approximated forms of the solutions (20). This part of research is the quite important theme of next publications.

VII. Conclusion

The new approach for computing the heteroclinic splitting via the matricant method is constructed. The corresponding approximate numerical technique of this method implementation is proposed. The example of the method application is given in the framework of the task of the gyrostat-spacecraft attitude dynamics. The generalized form of the function of detecting splitted manifolds intersections/contacts (analogous to the Melnikov's [1] and to the Wiggins' function [5]) is developed.

References

[1] Melnikov V.K. (1963), On the stability of the centre for time-periodic perturbations, Trans. Moscow Math. Soc. No.12, pp.1-57.
[2] Arnold V.I. (1964), Instability of dynamical systems with several degrees of freedom, Doklady Akademii Nauk SSSR, 156(1), pp.9-12.
[3] Kozlov V.V. (1980), Methods of qualitative analysis in the dynamics of a rigid body, Gos. Univ., Moscow.
[4] Holmes P. J., Marsden J. E. (1983), Horseshoes and Arnold diffusion for Hamiltonian systems on Lie groups, Indiana Univ. Math. J. 32, pp.273-309.
[5] Wiggins S. (1988), Global Bifurcations and Chaos: Analytical Methods (Applied mathematical sciences : vol. 73). Springer-Verlag.
[6] Doroshin A.V. (2017), Attitude dynamics of gyrostat-satellites under control by magnetic actuators at small perturbations, Communications in Nonlinear Science and Numerical Simulation 49, pp.159–175.
[7] Gantmakher, F.R. (1998), The theory of matrices (Vol. 131). American Mathematical Soc.

ISBN: 978-988-14047-8-7
ISSN: 2078-0958 (Print); ISSN: 2078-0966 (Online)